Journal of NeuroVirology, 11: 11–22, 2005

ISSN: 1355-0284 print / 1538-2443 online
DOI: 10.1080/13550280590900454

Taylor & Francis
Taylor & Francis Group

Characterization of West Nile viral replication and maturation in peripheral neurons in culture

Elizabeth Hunsperger and John T Roehrig

Division of Vector-Borne Infectious Diseases, Centers for Disease Control and Prevention, Public Health Service, Department of Health and Human Services, Fort Collins, Colorado, USA

The North American West Nile virus (WNV), New York 1999 strain, appears to be highly neurotropic, and its neuroinvasiveness is an important aspect of human disease. The authors have developed an *in vitro* model to study WNV replication and protein processing in neurons. They compared WNV infection of the dorsal root ganglion (DRG) neurons (sensory neurons) and PC-12 cells (sympathetic neurons) to WNV infection of the mosquito cell line, C6/36, and Vero cells. WNV infection of both neuronal cell types and C6/36 cells was not cytopathic up to 30 days post infection, and continual viral shedding was observed during this period. However, WNV infection of Vero cells was lytic. Interestingly, WNV infection of neurons was not efficient, requiring a high multiplicity of infection of $\geq$10. Indirect immunofluorescence assays using normal and confocal microscopy with flavivirus-reactive antibodies and WNV-infected neurons demonstrated viral antigen mostly associated with the plasma membrane and in the neurite processes. Treatment of WNV-infected C6/36, PC-12, or DRG cells with brefeldin A (BFA; a *trans*-Golgi inhibitor) or nocadazole (a β-tubulin inhibitor) had little effect on viral maturation and secretion. Treatment of WNV-infected Vero cells with BFA resulted in a 1000-fold decrease in viral titer, but nocodazole had no effect. Our studies suggest that even though PC-12 and DRG neurons are mammalian cells, viral protein processing and maturation in these cells more closely resembles replication in C6/36 insect cells than in mammalian Vero cells. *Journal of NeuroVirology* (2005) **11,** 11–22.

Keywords: brefeldin A; dorsal root ganglion; neurons; nocodazole; persistence; West Nile virus (WNV)

Introduction

West Nile virus (WNV) is a member of the family *Flaviviridae* of arthropod-borne, single-stranded, positive-sense RNA viruses that was first isolated from a febrile woman in Uganda in 1937 (Smithburn *et al*, 1940). The virus is maintained in nature in a cycle involving a mosquito vector and an avian amplifying host with humans as a dead-end incidental hosts. WNV belongs to the flavivirus serocomplex that includes St. Louis encephalitis, Japanese encephalitis, Murray Valley encephalitis, and Kunjin viruses. The WNV genome is approximately 11 kb in length with a single open reading frame of approximately 10 kb. As the viral polypeptide is synthesized, proteins are co- or post-translationally processed into structural (envelope, prM, and capsid) and nonstructural (NS1, NS2A, NS2B, NS3, NS4A, NS4B, and NS5) proteins. All of the nonstructural proteins have been implicated in viral RNA synthesis or protein processing at some level (reviewed in Brinton, 2002).

WNV has recently emerged as an important public health problem in the United States following its introduction into the New York City area in 1999 with 4156 confirmed human cases and 284 fatalities in 2002 (Anderson *et al*, 1999; Briese *et al*, 1999; Lanciotti *et al*, 1999; Nash *et al*, 2001; O'Leary *et al*, 2004). Phylogenetic analysis of WNV, groups

Address correspondence to Elizabeth A. Hunsperger, PhD, Centers for Disease Control and Prevention (CDC), National Center for Infectious Diseases, Division of Vector-Borne Infectious Diseases, P.O. Box 2087, Foothills Campus, Fort Collins, CO 80522, USA. E-mail: enh4@cdc.gov
Received 12 May 2004; accepted 2 September 2004.

strains into two distinct lineages of which the newly emerged North American (NY99) strain belongs to lineage 1 (Lanciotti *et al*, 2002). Only lineage 1 WNV are associated with human epidemics of neuroinvasive disease. Additionally, the North American strain was found to be highly neuroinvasive in *in vitro* studies that compared phenotype to genotype of 19 strains of WNV (Beasley *et al*, 2002). We have developed an *in vitro* model to study WN-NY99 viral replication and maturation in primary terminally differentiated neurons. Given that cerebral edema or encephalitis in WNV-infected people can be fatal, understanding the mechanism of viral invasion of the central nervous system (CNS) and the susceptibility of neurons to viral infection need to be better elucidated.

Previous reports suggest that flaviviruses access the CNS primarily through the olfactory bulb or directly through a blood brain barrier breakdown (Monath *et al*, 1983). Although both of these routes of CNS invasion may be possible, alternate routes of entry into the CNS have not been investigated. Based on human pathology, WNV is consistently detected in distinct regions of the brain including the medulla and thalamus (Sampson and Armbrustmacher, 2001). These observations suggest that WNV could also gain access to the CNS via the peripheral nervous system (PNS) and then to the brain stem via retrograde transport of virus by the neurons. This route of CNS invasion is consistent with the observation that the structures of the brain most affected by WNV have direct connections to either the sympathetic nervous system or the sensory nervous system. In addition, the initial inoculation of the virus by a virus-infected mosquito is in the dermal epithelium, which is highly enervated by sensory neurons. Moreover, because humans do not normally have a high or sustained viremia, it is less likely that neuroinvasion occurs through a blood-brain barrier breakdown (Biggerstaff and Petersen, 2002). Our initial studies have focused on determining the susceptibility to and replication of WNV in peripheral neurons *in vitro* to begin to assess the potential relevance of neuronal retrograde transport of virus.

To better understand WNV replication in peripheral neurons, we compared WNV neuronal replication and maturation in PC-12 cells (sympathetic neurons) and dorsal root ganglion (DRG) cells (sensory neurons) to WNV replication in the better characterized mammalian cell line, Vero, and the mosquito cell line C6/36. These experiments have determined that WNV infection in both neuronal cell types is similar to infection of C6/36 cells, a persistent-type infection demonstrating no cytopathic effects (CPEs). Furthermore, disruption of the Golgi apparatus with brefeldin A (BFA) following viral infection demonstrated that Vero cells required intact Golgi for proper viral secretion and maturation, whereas C6/36, PC-12, and DRG cells did not. However, disruption of microtubules with nocodazole following infection did not affect WNV replication in all cell types. Confocal microscopy experiments verified these results, supporting the conclusion that viral maturation in primary neurons resembles maturation in the mosquito cell line (C6/36).

Results

WNV establishes a nonlytic infection in PC-12 and DRG neurons that is MOI dependent

WNV infection of both PC-12 and DRG neurons required an multiplicity of infection (MOI) of at least 10. Lower MOI of 1 and 5 did not produce a productive primary infection. This inefficient WNV infection of neuronal cells was unusual compared to Vero cells that required an MOI ≤ 1 for successful WNV infection. Peak viral titers for DRG neurons was 4×10^3 plaque-forming units per milliliter (pfu/ml) (MOI = 10) and for PC-12 cells was 2.8×10^5 pfu/ml (MOI = 10) at 24 h post infection (p.i.) (Figure 1A). WNV-infected PC-12 cells maintained at least a 10-fold higher viral titer than the DRG neurons throughout the experimental time course. Growth curve analyses of both neuronal subtypes demonstrated a decrease in viral secretion 7 to 8 days p.i. At 8 days p.i., the cells were washed thoroughly to remove all viral particles from the medium and reassayed for the next 72 h for newly secreted infectious particles. Twenty-four hours after washing, viral titers rebounded indicating continued viral secretion.

WNV infection in DRG neurons was followed for a maximum of 92 days and the PC-12 cells were followed for 14 days. Infected DRG neurons demonstrated continual viral shedding throughout the 92-day time course and viral titers decreased over the time course (Figure 1C). During this prolonged infection, the DRG and PC-12 neurons displayed no apparent CPEs; however, the DRG neurons were senescing in culture after 3 months. These results were similar to those observed with WNV-infected C6/36 cells (data not shown). However, undifferentiated PC-12 cells did not replicate or secrete WNV following infection at the same MOIs tested for the differentiated cells.

WNV-infected Vero cells obtained a maximum viral titer of 1×10^9 pfu/ml at 48 h p.i (Figure 1B). Viral infection in Vero cells was lytic and the cells were dead by 48 h p.i. Viral release in all four cell types indicated that DRG, PC-12, and C6/36 cells had similar growth kinetics with a slow and gradual increase in viral titers within the first 48 h of infection. Conversely, Vero cells demonstrated a sharp increase in viral titer from 14 to 48 h p.i., demonstrating the rapid replication capabilities of WNV in this cell type (Figure 1B).

Immunoblot analyses identified differing temporal viral protein expression in all cell types

Proteins from WNV-infected Vero, C6/36, PC-12, and DRG cells were analyzed by sodium dodecyl

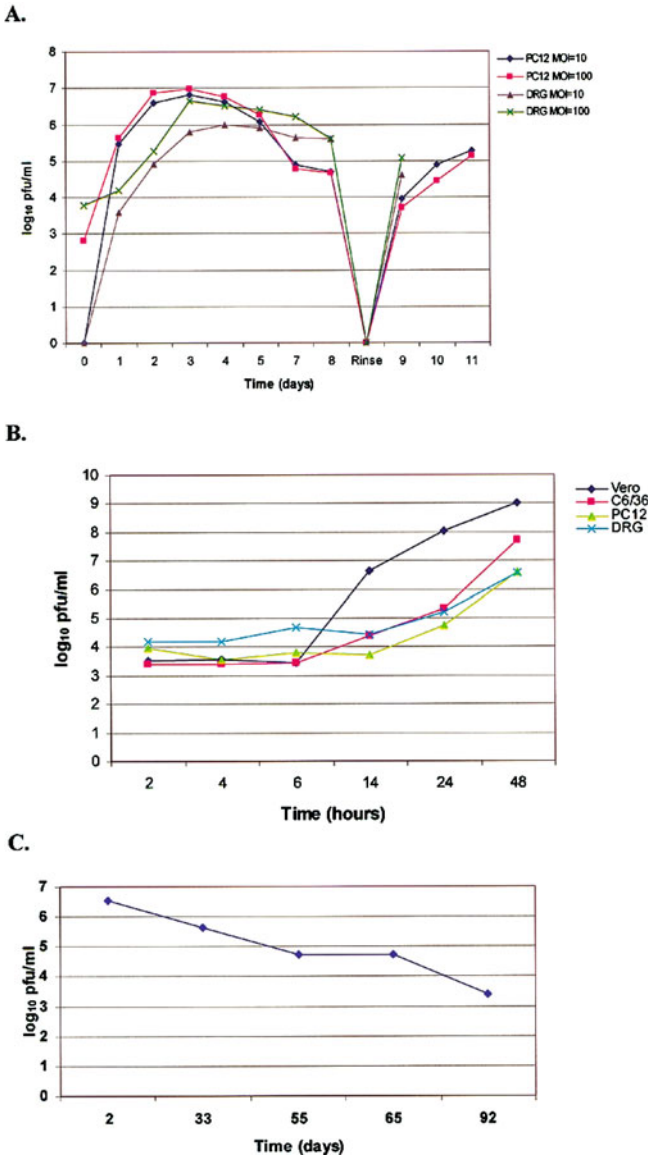

Figure 1 (**A**) WNV growth curves in primary DRG neurons and PC-12 cells. Both neuronal subtypes were infected with either MOI = 10 or 100 pfu/cell and the medium was assayed for infectious viral particles using a standard plaque assay. After day 8 the neurons were washed 3 times with normal culturing medium and infectious virus was assayed for the final rinse and 72 h after the rinse. MOI of 1 and 5 produced no infectious virus. (**B**) WNV growth curve comparisons for Vero, C6/36, DRG, and PC-12 cells. Specimens were taken at 2, 4, 6, 14, 24, and 48 h p.i. The medium was assayed for infectious viral particles using a standard plaque assay. (**C**) Long-term WNV growth curve in DRG neurons. DRG neurons were infected with WNV at MOI = 100 and aliquots of medium were harvested for plaque assay analysis during the indicated time points.

sulfate (SDS)-polyacrylamide gel electrophoresis and immunoblotting. Although cellular protein backgrounds were high in these immunoblots, the presence of viral proteins could be ascertained based on molecular mass and comparisons to mock-infected cells. Viral proteins could be detected by 12 h p.i. in WNV-infected Vero cells (Figure 2A). There was a steady increase in the glycosylated form of viral structural protein E (55 kDa). A protein band at 36 kDa corresponded to the predicted size of the nonglycosylated form of the NS1 protein. Protein bands at approximately 25 kDa and 23 kDa corresponded to glycosylated and nonglycosylated prM proteins, respectively, and two other bands (approximately 12 kDa and 8 kDa) were presumed to be the C and M proteins, respectively. These smaller bands appeared to intensify at 20 h p.i.

WNV proteins could also be detected at 14 h p.i. in virus-infected C6/36 cells (Figure 2B). At this time point, viral protein E, NS1, and NS3 were detected. Another faint band at approximately 10 to 12 kDa observed after 48 h p.i. likely represents the capsid protein.

WNV NS3, E, and C proteins could be detected in virus-infected PC-12 cells at 24 h p.i. (Figure 2C). Similarly, viral proteins (including NS1) were detected in the DRG lysates at 24 h p.i. NS3 and E were consistently resolved in these protein gels when probed with the polyclonal anti-WNV antibody. The prM protein could not be readily detected in WNV-infected DRG neurons. At 48 h p.i. there was evidence of a larger band (molecular mass of 12 kDa) that may represent the capsid protein (Figure 2D).

WNV release from neurons and C6/36 cells is insensitive to BFA treatment

To further characterize viral replication in the neuronal cells, we treated virus-infected cells with the Golgi inhibitor BFA and then measured differences in intracellular and extracellular virus. The Golgi apparatus is hypothesized as an essential organelle for viral protein trafficking and encapsidation of nascent genomic RNA, budding of nascent virions, and eventual movement of nascent virions to the cell surface (reviewed in Brinton, 2002). In theory, BFA-induced disruption of the Golgi apparatus should inhibit virus maturation and correspondingly reduce the amount of virus released (Dinter and Berger, 1998). It has been shown previously that BFA does not affect flaviviral replication in C6/36 cells, but it does reduce viral replication in mammalian-derived cells (Sreenivasan *et al*, 1993).

WNV replication and maturation in DRG neurons, PC-12 cells, and C6/36 cells was relatively insensitive to a 20-h treatment with BFA as determined by measuring free and cell-associated virus (Figure 3). There was approximately a 0.5 $\log_{10}$ decrease in extracellular virus following BFA treatment of PC-12 or DRG cultures compared to uninfected control cells, this difference was not significant (Figure 3A). Cell-associated WNV titers in BFA-treated DRG neurons or PC-12 cells were reduced only about 10-fold (Figure 3B). However, in Vero cells there was a 1000-fold decrease in both cell-associated

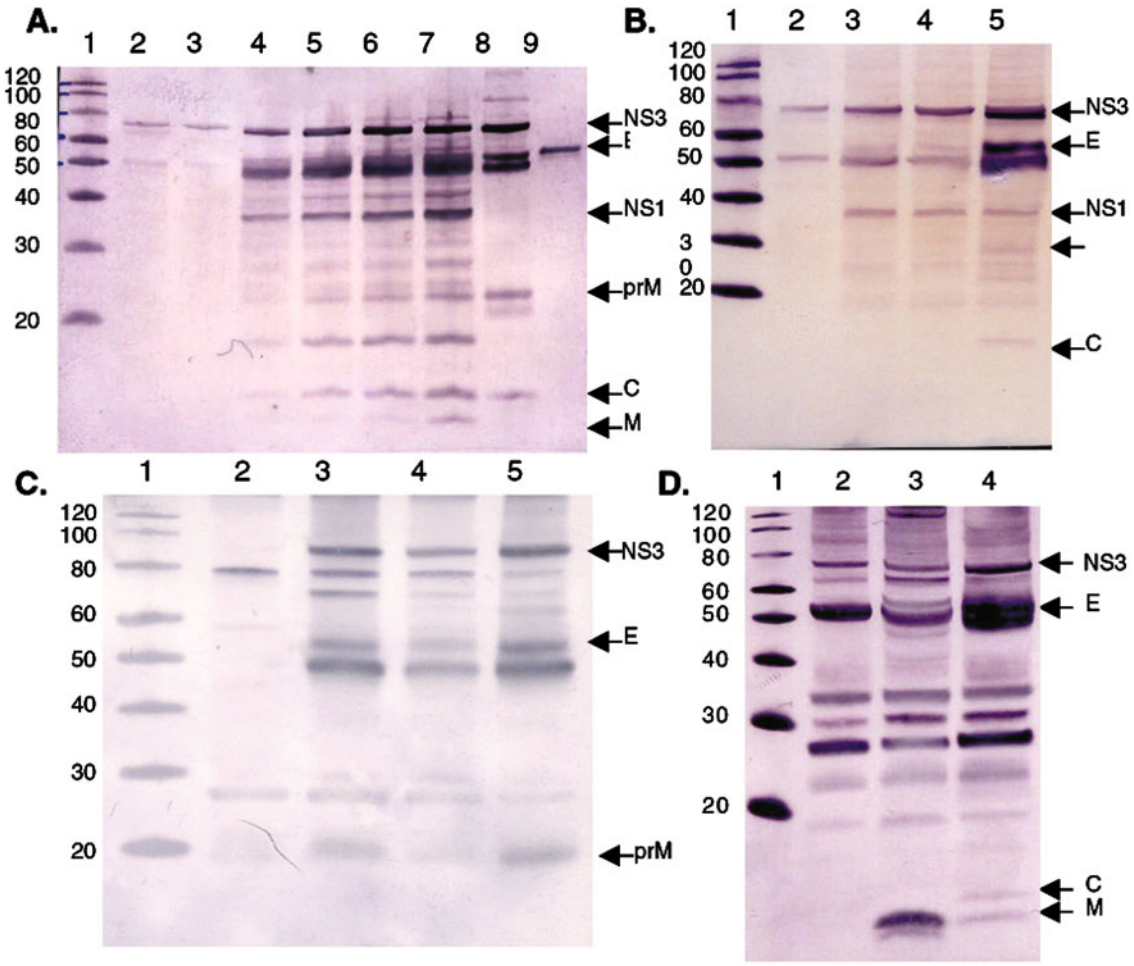

Figure 2 Protein expression in the lysate of WNV-infected Vero, C6/36, PC-12, and DRG cells. (**A**) Immunoblotting of WNV viral antigens expressed in infected Vero cell lysate. Lane 1, molecular weight markers; lane 2, mock infected; lane 3, 6 h p.i. WNV; lane 4, 12 h p.i. WNV; lane 5, 16 h p.i. WNV; lane 6, 18 h p.i. WNV; lane 7, 20 h p.i. WNV; lane 8, 48 h p.i.; lane 9, purified WNV. (**B**) WNV-infected C6/36 cell lysate. Lane 1, molecular weight markers; lane 2, mock infected; lane 3, 14 h p.i. WNV; lane 4, 24 h p.i. WNV; lane 5, 48 h p.i. WNV. (**C**) WNV protein expression in infected PC-12 cell lysate. Lane 1, molecular weight marker; lane 2, mock infected; lane 3, 24 h p.i. WNV; Lane 4, 48 h p.i. WNV; lane 5, 96 h p.i. WNV (**D**) WNV protein expression in WNV-infected DRG lysate. Lane 1, molecular weight markers; lane 2 mock infected; lane 3, 24 h p.i. WNV; lane 3, 48 h p.i. WNV.

and extracellular virus following treatment with either 1 or 10 μg/ml of BFA.

WNV release from all cell types is not affected by nocodazole treatment

In order to determine whether microtubule-based transport systems were necessary for WN viral secretion or viral protein trafficking, we used nocodazole. Nocodazole is an antimitotic agent that disrupts microtubules by binding to β-tubulin and preventing the formation of one of the two disulfide linkages, and resulting in cell cycle arrest (Jordan *et al*, 1992). Although this effect is not relevant for postmitotic cells such as the neurons, it may be a crucial aspect of replication in actively dividing cells such as Vero and C6/36 cells. Unlike BFA treatment, nocodazole treatment of WNV-infected DRG, Vero, C6/36, and PC-12 cells had no effect on the amount of cell-associated or free virus (Figure 4A and B).

Immunofluorescence demonstrates the presence of WNV antigens in neurite processes in PC-12 cells

The intracellular location of WNV antigens in infected PC-12 cells was determined using immunofluorescence. Viral antigens were observed in the cell bodies mostly concentrated along the plasma membrane as well as throughout the neurite processes when probed with an anti-WNV polyclonal antibody (see Figure 6E and F). Viral antigens were never observed in the nucleus of these cells. Staining of these cells with an E protein–specific monoclonal antibody (3.91D) determined that much of the viral antigen identified in the neurite processes was E protein (data not shown). Negative controls included infected PC-12 cells treated with secondary antibody only and mock-infected PC-12 cells probed the same as infected cells. Both of these controls yielded no fluorescence (data not shown).

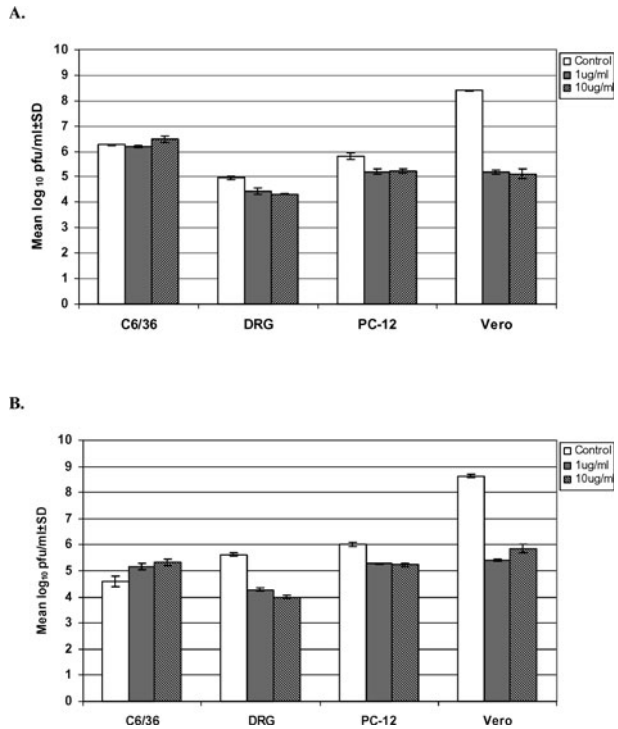

Figure 3 Effects of BFA treatment on production of progeny virus. (**A**) Infectious virus assayed from the medium of BFA- (1 and 10 μg/ml) treated WNV-infected C6/36, DRG, PC-12, and Vero cells after 20 h. Standard plaque assays were used to determine pfu/ml. (**B**) Infectious virus in the cell lysate from BFA-treated WNV-infected C6/36, DRG, PC-12, and Vero cells following 20 h of infection.

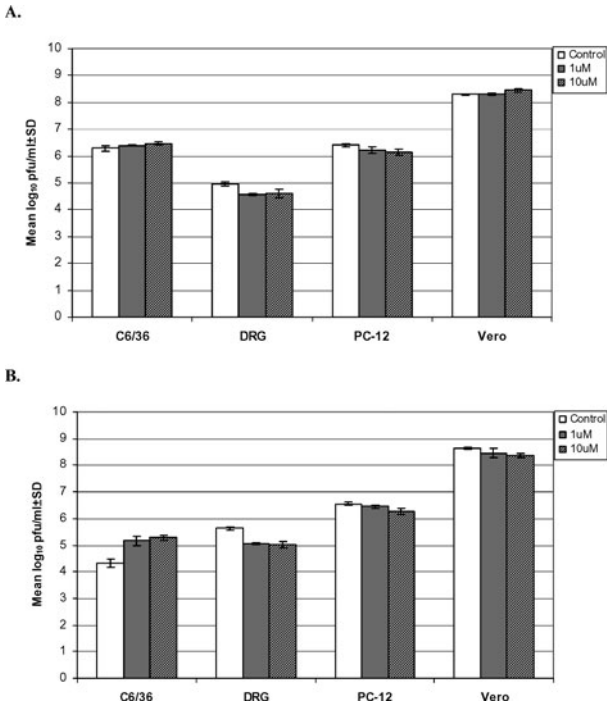

Figure 4 Effects of nocodazole treatment on the production of progeny virus. (**A**) Infectious virus assayed from the medium of nocodazole- (1 and 10 μM) treated WNV-infected C6/36, PC-12, DRG, and Vero cells. (**B**) Infectious virus in the cell lysate from nocodazole (1 and 10 μM) treated WNV-infected C6/36, DRG, PC-12, and Vero cells following 20 h of infection. Standard plaque assays were used to determine pfu/ml.

Intracellular localization of WNV antigens in DRG, PC-12, C6/36, and Vero cells and their redistribution following treatment with BFA or nocodazole

Using confocal microscopy, we determined the cellular location of viral antigens following a WNV primary infection in all cell types. In both cultured DRG neurons (Figure 5B) and PC-12 cells (Figure 6B), viral antigens were primarily located adjacent to the plasma membrane at 24 h p.i., and viral antigen was not as tightly organized in PC-12 cells as compared with DRG neurons (Figures 5B and 6B). Viral antigens were often observed in the DRG neurite processes (Figure 5B). In WNV-infected Vero cells, antigen localization was perinuclear (Figure 7A). Unlike the neurons and the Vero cells, viral antigen expression in C6/36 cells was punctate in vesicle-like packages distributed throughout the cytoplasm (Figure 8A). In all cell types tested no viral antigen was found in the nucleus.

Interestingly, viral antigen distribution was altered in the presence of BFA and nocodazole in some cell types. In WNV-infected Vero cells, the normal perinuclear distribution of viral antigens (Figure 7A) was less organized and more dispersed throughout the cytoplasm following BFA treatment (Figure 7B). In some cells, punctate staining in the cytoplasm was observed, suggesting that viral antigens may have been trapped in specific cellular compartments (Figure 7B). Because nocodazole treatment causes cytoskeletal rearrangement, there was a reduction in the β-tubulin (Cy3) staining with less distinct microtubule projections. Nevertheless, the viral antigens remained mostly perinuclear similar to the control WNV-infected cells, a result that was consistent with the plaque assays results (Figure 7C). In the C6/36 cells, viral antigens were distributed throughout the cytoplasm as distinct punctate regions at 24 h p.i. (Figure 8A) and this distribution did not change in the presence of either BFA (Figure 8B) or nocodazole (Figure 8C). These results confirmed the plaque assay results.

WNV antigen distribution in DRG neurons was unchanged by treatment with BFA (Figure 5C). With nocodazole treatment, however, DRG cells no longer appeared to express viral antigen in the neurite processes, possibly indicating that the β-tubulin block had inhibited the viral antigen movement along the processes (Figure 5D). Additionally, the viral antigen distribution in the cytoplasm changed from an even distribution along the plasma membrane to vesicular staining throughout the cytoplasm. Although these observations suggest that nocodazole changed cellular localization of WNV antigens in DRG neurons, the plaque assay results did not reflect any major differences between treated and untreated controls. In BFA-treated, WNV-infected PC-12 cells, viral antigen

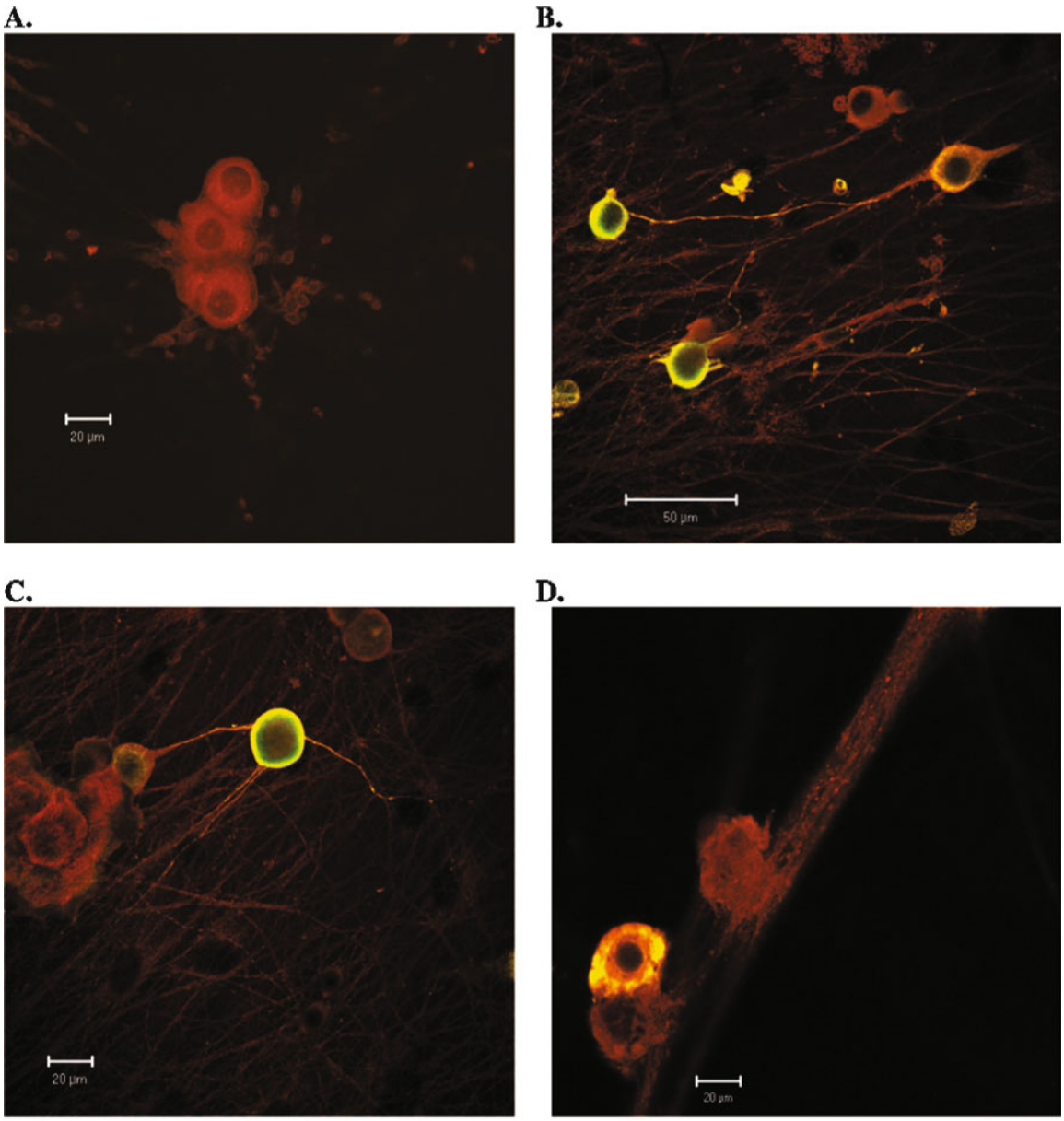

Figure 5 Confocal microscopic analyses of antigen distribution in WNV-infected DRG neurons at 24 h p.i. The neurons were probed with a primary polyclonal antibody (MHIAF) directed against WNV antigens and a secondary antibody conjugated to FITC. The cells were counterstained with a β-tubulin monoclonal antibody conjugated to Cy3. (**A**) Mock-infected DRG neurons; scale bar = 20 μm. (**B**) DRG neurons infected with WNV; scale bar = 520 μm. (**C**) WNV-infected DRG neurons treated with 10 μg/ml; scale bar = 20 μm. (**D**) Nocodazole-(10 μM) treated WNV-infected DRG neurons, scale bar = 20 μm.

was distributed in what appeared to be inclusion bodies or vesicles (Figure 6D), and in the nocodazole-treated PC-12 cells, viral antigens localized to perinuclear regions rather than the plasma membrane (Figure 6C).

Discussion

Neurons are important human target cells during a WNV infection. Neuronal toxicity in the CNS during a WNV infection causes devastating effects in humans, including encephalitis, paralysis, and sometimes death (reviewed by O'Leary *et al*, 2004). The sequela of a primary WNV infection can last for years, with some of the acute paralysis developing into chronic neurological dysfunction (Sejvar *et al*, 2003). To address the effects of a WNV infection in neurons, we characterized viral replication in peripheral primary neurons in culture. Previous characterization of WNV infection has been performed in stem cells or cell lines that were differentiated to neuron-like cells but were not primary neurons (Shrestha *et al*, 2003). This is the first time that

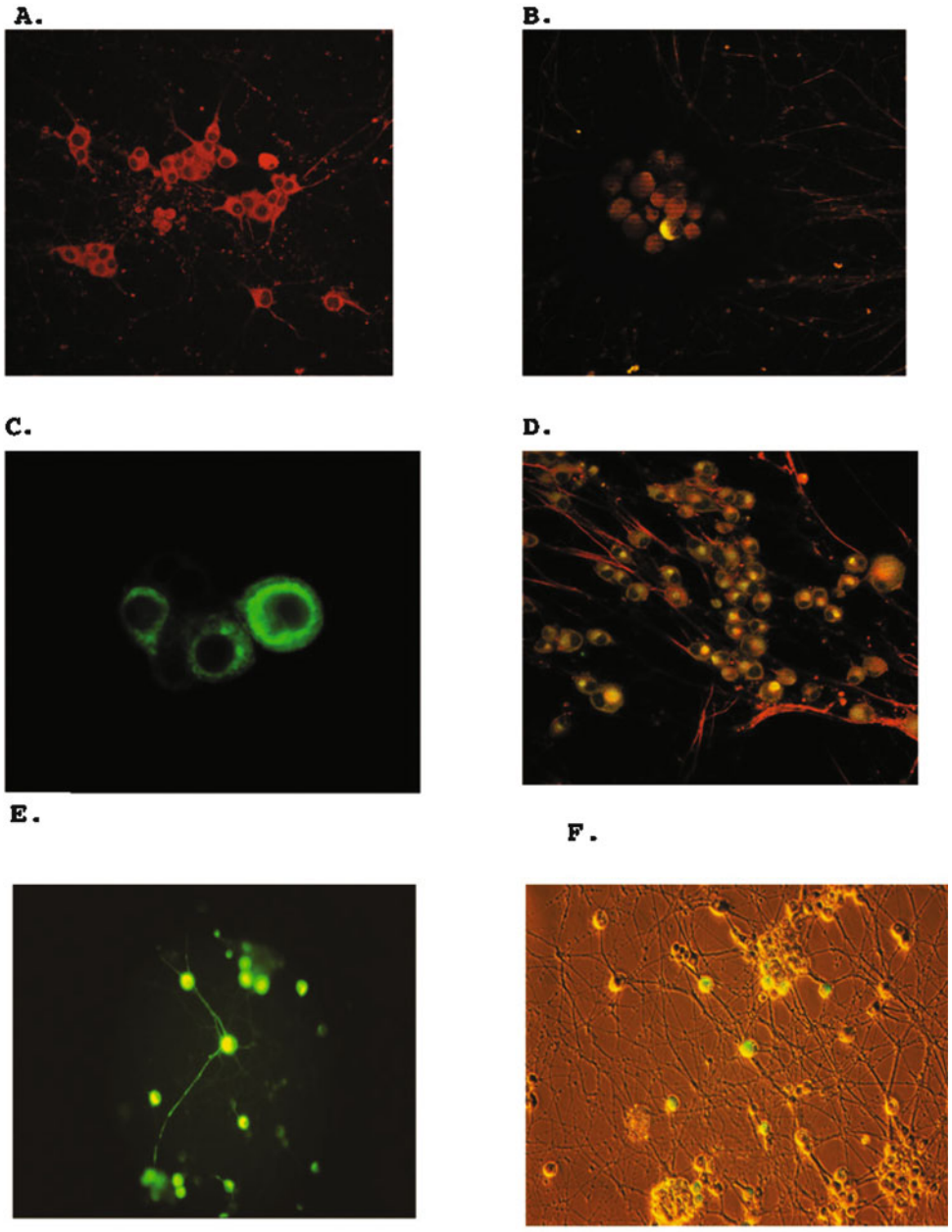

Figure 6 Confocal microscopic analyses of antigen distribution in WNV-infected PC-12 cells at 24 h p.i. Primary polyclonal antibody directed against WNV (MHIAF) and visualized with a secondary antibody conjugated to FITC. The cells were counterstained with β-tubulin monoclonal antibody conjugated to Cy3. Scale bar of 20 μm for all images. (**A**) Mock-infected cultures; (**B**) WNV-infected PC-12 cells; (**C**) nocodazole-(10 μM) treated WNV-infected PC-12 cells; (**D**) BFA. (10 μg/ml) treated WNV-infected PC-12 cells. (**E**) IFA analysis of viral antigen distribution in WNV-infected PC-12 cells. Immunofluorescence of WNV-infected PC-12 cells stained with MHIAF polyclonal antibody for WNV viral antigens. (**F**). Light microscopy of the same field that the fluorescent image was obtained.

terminally differentiated primary sensory neurons have been used to investigate WNV infection. Our results determined that WNV can replicate in both sensory and sympathetic neurons of the PNS *in vitro*, and that WNV replication in PC-12 and DRG cells more closely mimic WNV replication in the mosquito cell line, C6/36, than the mammalian Vero cell line. Both viral replication rates and protein synthesis kinetics in PC-12 and DRG neurons were similar and were slower than in Vero cells (Figure 1B and 2). Interestingly, undifferentiated PC-12 cells were not susceptible to WNV infection, which may indicate that prior to differentiation these cells do not express the host cell receptor that mediates viral entry via endocytosis. However, in the presence of nerve growth factor (NGF) following differentiation, the cells become permissive to WNV infection, replicating and secreting virus readily. Currently, there is little known about the host receptor for flaviviruses on neuronal cells.

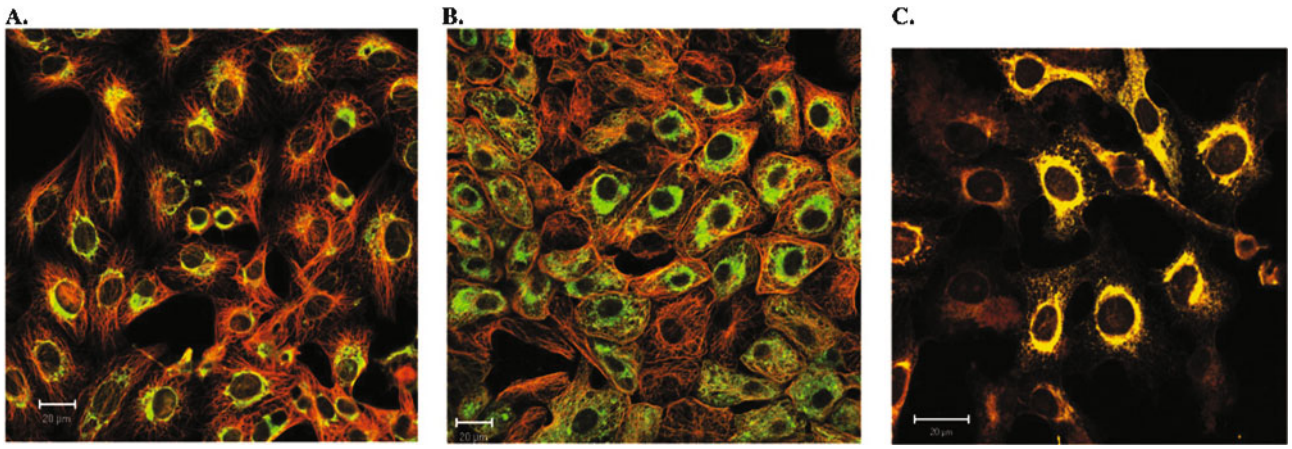

Figure 7 Confocal microscopic analyses of antigen distribution in WNV-infected Vero cells at 24 h p.i. Primary polyclonal antibody directed against WNV (MHIAF) and visualized with a secondary antibody conjugated to FITC. The cells were counterstained with β-tubulin monoclonal antibody conjugated to Cy3. All images contain a 20 μm scale bar. (**A**) WNV-infected cells; (**B**) WNV-infected cells treated with BFA (10 μg/ml); (**C**) WNV-infected cells treated with nocodazole (10 μM).

Characterization of viral infectivity p.i. demonstrated that these neurons cannot be 100% infected despite a high MOI. The reason for this is unknown. At lower MOI of 1 and 5, the neurons failed to be infected. Because viral infectivity in the neuron is inefficient, this may account for the lower peak viral titers compared to WNV-infected Vero cells. Furthermore, analysis of plaque morphology throughout the infection period indicated a trend towards smaller plaques at the later time points of infection (days 7 to 9), suggesting some type of neuronal cell culture adaptation (data not shown). Genomic sequencing of virus recovered from persistently infected cells will provide more information about viral adaptation in these cultured cells.

The DRG neurons cells are not killed by WNV infection, secreting virus for up to 92 days p.i. (Figure 1C). This persistent infection is similar to what was observed in C6/36 cells infected with St Louis encephalitis and flavivirus-resistant mouse embryofibroblasts infected with WNV (Brinton, 1981; Randolph and Hardy, 1988). Furthermore, persistence of WNV was previously observed in infected Rhesus monkeys. The duration of persistence in these animals was $5\frac{1}{2}$ months following the initial infection (Pogodina *et al*, 1983). Unlike an acute infection, in a persistent infection there is continual shedding of virus and often virus replication is attenuated by the production of defective interfering particles and the interferon response. The persistent infection established in the culture system appears to be chronic because the cells survived over 90 days in culture and continually secreted infectious virus. Whether WNV establishes a persistent versus lytic infection *in vivo* could be based on the maturation pathway of the virus, therefore we investigated this process in all cell types.

Flavivirus maturation and protein trafficking normally require an intact Golgi apparatus and microtubule system (reviewed by Brinton, 2002).

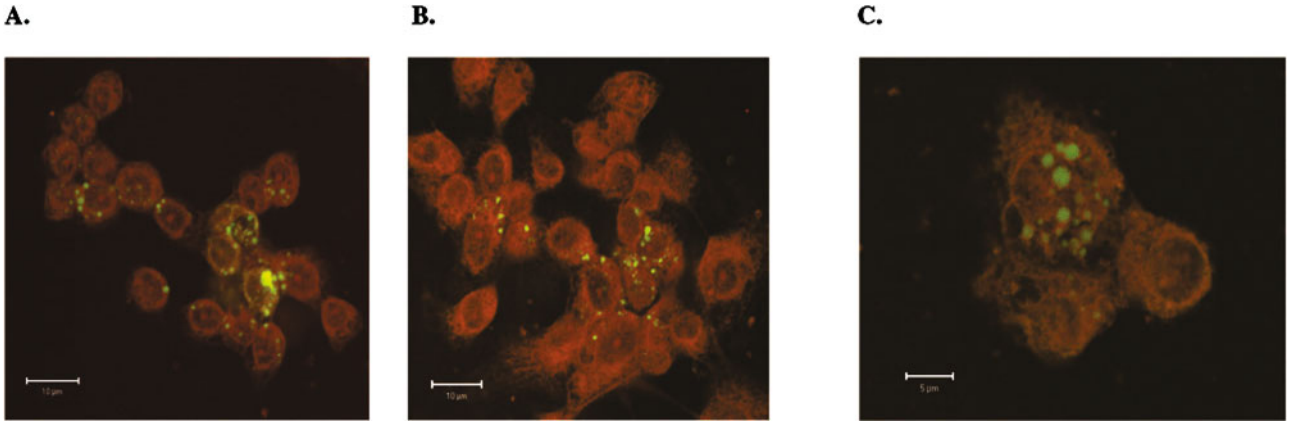

Figure 8 Confocal microscopic analyses of antigen distribution in WNV-infected C6/36 cells at 24 h p.i. Primary polyclonal antibody directed against WNV (MHIAF) and visualized with a secondary antibody conjugated to FITC. The cells were counterstained with β-tubulin monoclonal antibody conjugated to Cy3. (**A**) WNV-infected cells; (**B**) WNV-infected cells treated with BFA (10 μg/ml); (**C**) WNV-infected cells treated with nocodazole (10 μM).

Disruption of the Golgi with BFA treatment in normal dividing cells affects the forward transport of protein processing starting from the *cis*-Golgi to the *trans*-Golgi (Vetterlein *et al*, 2003). Flavivirus maturation is presumed to require the *trans*-Golgi where the host cellular protein, furin, cleaves the viral structural protein prM to M, its final mature form (Elshuber *et al*, 2003; Stadler *et al*, 1997). However, in dengue virus–infected C3/36 cells, viral particles are released with a high proportion of prM, yet these virions were still infectious (He *et al*, 1995). Clearly, not all flaviviruses utilize the same mechanism of protein processing and these differences are likely to be cell-type specific.

Results from WNV protein trafficking disruption experiments using BFA also suggest that viral maturation differs significantly between neurons and Vero cells and is more similar to C6/36 cells. The neuronal and C6/36 cells were not affected by BFA treatment, suggesting that both cells follow similar maturation process which differs from Vero cells. Interestingly, prM could be detected in WNV-infected PC-12 cells, but not in WNV-infected DRG neurons. If the *trans*-Golgi is required for appropriate cleavage of the structural protein prM to M and packaging of mature infectious viral particles into endosomes for viral release, then BFA treatment should have decreased secretion of infectious viral particles. However, only WNV-infected Vero cells showed a decrease in viral secretion (1000-fold) following BFA treatment. In Vero cells, viral maturation was also inhibited by BFA treatment because infectious cell-associated virus particles were reduced when compared to virus-infected untreated control cells. This implies that the *trans*-Golgi is required to assemble infectious viral particles and also for viral secretion by infected Vero cells as previously observed (Sreenivasan *et al*, 1993). Additionally, previous studies on the replication of Kunjin (a genetically related flavivirus) in Vero cells demonstrated an association of Kunjin RNA with *trans*-Golgi structures and disruption of this structure using BFA caused a reduction of viral secretion similar to our observations (Mackenzie *et al*, 1999; Mackenzie and Westaway, 2001).

Confocal microscopy experiments confirmed these growth results. BFA treatment resulted in redistribution of viral antigens throughout the cytoplasm of WNV-infected Vero cells when compared to the tightly assembled perinuclear staining of the WNV-infected control cells (Figure 7). BFA treatment had no effect on the distribution of viral antigen within the cytoplasm of WNV-infected PC-12, DRG, or C6/36 cells (Figure 5C, 6D, and 8B). These results again show that WNV infection of C6/36 cells and neurons follow similar viral maturation pathways.

In order to determine whether all four cell types relied on microtubules for efficient viral secretion or transport, we treated the cells with the microtubule inhibitor, nocodazole. Nocodazole disrupts microtubules by binding to β-tubulin and preventing the formation of one or two disulfide linkages (Vasquez *et al*, 1997). Because both confocal and immunofluorescence microscopy showed that viral antigens were present along the neurite processes, we speculated that microtubule motors were important for viral transport. Many other viruses utilize microtubule motors for egress and transport in cells (Mabit *et al*, 2002; Moss and Ward, 2001; Raux *et al*, 2000). Previous reports suggest that WNV Sarafend strain prefers egress from the apical side of polarized Vero cells and the release of Kunjin virus had no preference between apical and basal (Chu and Ng, 2002). DRG neurons are considered pseudounipolar cells. If WNV required microtubule motors for transport, then inhibition of microtubule transport should decrease virus release and perhaps prevent retrograde transport of the virus from peripheral neurons to the CNS *in vivo*.

Plaque assay experiments indicated that inhibition of microtubule dynamics with the β-tubulin inhibitor nocodazole did not change overall levels of viral secretion in C6/36, PC-12, DRG or Vero cells; however, confocal microscopy demonstrated a difference in antigen distribution in WNV-infected PC-12 and DRG neurons compared to WNV-infected control cells. For nocodazole-treated DRG cultures, the staining pattern changed from a uniform staining along the plasma membrane to a punctate staining pattern throughout the cytoplasm. In PC-12 cells, viral antigen distribution was punctate similar to that observed in DRG neurons. Interestingly, viral antigens in PC-12 and DRG neurons were not detected along the neurite processes following nocodazole treatment as was observed in the untreated WNV-infected control cultures. These results suggest that the localization of viral antigens to the neurites in untreated control cells may by to occur via microtubule motor proteins.

Because standard IFA and confocal microscopy of virus-infected neurons demonstrated viral antigens in the neurite processes, retrograde transport of WNV between neurons as a mode for CNS invasion remains a possibility. Other RNA viruses, such as polio and rabies, access neurons that enervate infected tissue and are presumed to be mobilized via retrograde transport from the PNS to the CNS (Gromeier and Wimmer, 1998). Perhaps this phenomenon of PNS infection leading to CNS invasion occurs in a certain population of WNV-infected individuals, allowing virus to access the CNS and creating the encephalitic and poliomyelitis-like symptoms observed in humans (Solomon and Willison, 2003). Viruses capable of retrograde transport and trans-synaptic transport take advantage of the vulnerability of the PNS as a means for neuroinvasion.

In summary, we have demonstrated that neurons of the peripheral nervous system are capable of supporting a persistent, nonlytic WNV infection. Additionally, viral antigens were observed in the neurite processes and this localization appeared to be under microtubule motor control. Viral replication and

protein trafficking in neurons demonstrated many similarities to the insect cell line, C6/36. These similarities included a sustained infection that was not lytic, late expression of viral antigens, and insensitivity to Golgi disruption and nocodazole treatment. These studies infer that the mechanism of viral replication and protein processing in neurons is similar to C6/36 cells and that a mechanism of retrograde transport as an alternative mechanism for neuroinvasion of the CNS via the PNS is possible.

Materials and methods

Virus strain
The New York 1999 (NY99) strain of WNV used in these studies was obtained from the reference collection at the Division of Vector-Borne Infectious Diseases, Centers for Disease Control and Prevention (CDC; CDC, 1999). This WNV strain was isolated from an infected Chilean flamingo in the Bronx Zoo and was passaged once in suckling mice and twice in Vero cells (Lanciotti *et al*, 1999).

Cell culture
All the cell lines used in these studies were obtained from the American Type Culture Collection (ATCC). Vero (African green monkey kidney) cells were maintained in Dulbecco's modified Eagle medium (DMEM) supplemented with 10% fetal bovine serum (FBS) and 1% penicillin/streptomycin (Pen/Strep) in a 5% CO_2 incubator at 37°C. Because Vero cells are routinely used to propagate WNV in culture, the WNV growth curves from Vero cells are used as a positive control for comparison purposes between all the cells infected in these studies. The mosquito cell line, C6/36 (*Aedes albopictus* clone) cells were maintained in DMEM with 2% FBS, 1% nonessential amino acids, 1% sodium pyruvate, 2% sodium bicarbonate, and 1% Pen/Strep in a 5% CO_2 incubator at 28°C.

The PC-12 cell line (rat adrenal pheochromocytoma) were maintained in RPMI 1640 supplemented with 10% horse serum (HS), 5% FBS, 10 mM HEPES, 1 mM sodium pyruvate, 4.5 g/L glucose, and 1.5g/L bicarbonate (Invitrogen). The cells were differentiated into neuronal cells in the presence of 100 ng/ml NGF 2.5S and 1% HS and FBS supplemented medium (Invitrogen). The cells require 7 days for terminal differentiation. Upon differentiation, PC-12 cells undergo a G0 arrest state and changes in cellular morphology, including the development of neurite projections and the synthesis and storage of the catecholamine neurotransmitters, dopamine and norepinephrine, occurs. PC-12 cells are commonly used as a model to study neurobiology and neurochemistry and are often either characterized as a neuroendrocrine or sympathetic nervous system neurons following differentiation (Greene and Tischler, 1976).

DRG primary sensory neuronal cultures were isolated from embryonic day 16 rats as previously described (Smith and Wilcox, 1996). The ganglion were dissociated to a single-cell suspension and plated onto 24-well collagen-coated plates and cultured in N2 medium (DMEM/F12, 50 pg/ml NGF, and N2 supplement [Invitrogen]). The neurons were allowed to mature in culture for 21 days prior to infection with WNV virus. Following maturation, the neurons were infected with a MOI ranging from 1 to 100. Aliquots of 100 μl of medium was removed daily and assayed for infectious viral particles using a standard plaque assay in Vero cells.

Plaque assay detection of WNV in cell culture medium and lysate
C6/36 and Vero cells were infected at an MOI of 1 and at designated time points an aliquot of the medium was removed and stored at −80°C for plaque assays. PC-12 and DRG neurons were infected with WNV at varying MOI (1 to 100) and aliquots of the cell medium were assayed for infectious virus at indicated time points. Additionally, the cell lysate of these infected cells were also collected p.i. For lysate samples, the infected cells were washed two times with phosphate-buffered saline (PBS) following the specified time points, removed from the plates using a cell scraper, and lysed by freezing the cells at −80°C followed by a rapid thaw. Data points represent mean values for each cell type ($n = 4$).

To determine infectious virus in each sample, diluted infectious supernatant or lysate samples were adsorbed on Vero cells for an hour and then removed. An agarose overlay consisting of DMEM supplemented with 10% FBS, 1% L-glutamine, 1% Pen/Strep, 2% sodium bicarbonate, and 10% agarose was added to the cells following virus adsorption and incubated for 3 days. Following incubation, the agarose was removed and the cells were stained with 0.25% crystal violet in 40% methanol solution for plaque visualization. Plaques were counted for each sample dilution and plaque forming units per milliliter (pfu/ml) of sample were calculated.

Immunoblotting to identify WNV proteins in virus-infected cell lysates
WNV-infected PC-12, Vero, C6/36, and DRG cells were lysed at varying times p.i. with RIPA buffer (50 mM Tris-Cl, pH = 7.4, 150 mM NaCl, 1% Triton × 100, 1% sodium deoxycholate, 0.1% SDS) containing a protease inhibitor cocktail (Sigma). The lysates from each cell type were reduced using reducing agent (Invitrogen), boiled for 10 min, and electrophoresed in 10% Bis-Tris (Invitrogen) SDS-polyacrylamide gels for viral protein analysis. The proteins were transferred onto a nitrocellulose membrane and blocked overnight with 5% nonfat milk in Tris-buffered saline with 0.1% Tween-20 (TBS-T). The membranes were probed for 1 h at room temperature (RT) using a 1:200 dilution of anti-WNV mouse

hyperimmune ascites fluid (MHIAF; strain Ar248). Membranes were washed 3 times for 5 min each with TBS-T and then incubated with a 1:500 dilution of secondary antibody (goat anti-mouse immunoglobulin G [IgG] conjugated to alkaline phosphatase; Jackson Laboratories) for 1 h at RT. Following 3 washes with TBS-T for 5 min each, the proteins were visualized using the immunohistochemical substrate for alkaline phosphatase, BCIP/NBT (KPL).

Immunofluorescence and confocal microscopy of WNV antigen expression

DRG and PC-12 neurons were infected with WNV for either 1, 2, and/or 4 days and fixed with cold methanol for 10 min. C6/36 and Vero cells were infected with WNV for 24 h and fixed with cold methanol for 10 min. The cells were cultured on glass cover slips for all confocal microscopy experiments. Following fixation, the cells were washed with PBS and blocked with 2% goat serum in PBS with 0.1% Tween-20 (PBS-T) for 2 h or overnight. The cells were incubated with anti-WNV MHIAF (1:100 dilution) for 1 h and then washed 3 times with PBS-T for 10 min each and subsequently treated with goat anti-mouse IgG conjugated to fluorescein isothiocyanate (FITC) (Jackson Laboratories) for 30 min. Following three more washes with PBS-T, the cells were counter stained with a 1:500 dilution of anti-β-tubulin mouse monoclonal antibody conjugated to Cy3 (Sigma) for 30 min and washed 3 times each for 10 min with PBS-T. Controls for antibody specificity included a no primary antibody control and a mock-infected control. The cells were visualized either under fluorescent or confocal microscopy to determine the cellular location of viral antigens (Carl Zeiss, LSM-Pascal). Special attention was directed to the location of viral antigens in neurite processes and the association of these antigens with microtubules.

BFA and nocodazole treatment of PC-12, DRG, Vero, and C6/36 cells

The cells were infected with WNV for 1 h and subsequently treated with BFA at 1 and 10 μg/ml or nocodazole at 1 and 1 μM (Sigma). The cells were incubated with each compound for 20 h and then assayed for infectious virus in cell culture supernatants and in cell lysates ($n=6$ for each treatment group). The medium was removed for plaque assays after the 20-h time point and the cells were rinsed twice with PBS. Following the PBS rinses, the cells were resuspended in culture medium containing 10% DMEM, 1% Pen/Strep, and 2% sodium bicarbonate and placed in -80°C for a freeze-thaw cycle. Plaque assays were used to measure the mean pfu/ml $\pm$ standard deviation from each treatment group.

References

Centers for Disease Control and Prevention (1999). Update: West Nile Virus encephalitis—New York, 1999. *MMWR Morb Mortal Wkly Rep* **48:** 944–946, 955.

Anderson JF, Andreadis TG, Vossbrinck CR, Tirrell S, Wakem EM, French RA, Garmendia AE, Van Kruiningen HJ (1999). Isolation of West Nile virus from mosquitoes, crows, and a Cooper's hawk in Connecticut. *Science* **286:** 2331–2333.

Beasley DW, Li L, Suderman MT, Barrett AD (2002). Mouse neuroinvasive phenotype of West Nile virus strains varies depending upon virus genotype. *Virology* **296:** 17–23.

Biggerstaff BJ, Petersen LR (2002). Estimated risk of West Nile virus transmission through blood transfusion during an epidemic in Queens, New York City. *Transfusion* **42:** 1019–1026.

Briese T, Jia XY, Huang C, Grady LJ, Lipkin WI (1999). Identification of a Kunjin/West Nile-like flavivirus in brains of patients with New York encephalitis. *Lancet* **354:** 1261–1262.

Brinton MA (1981). Isolation of a replication-efficient mutant of West Nile virus from a persistently infected genetically resistant mouse cell culture. *J Virol* **39:** 413–421.

Brinton MA (2002). The molecular biology of West Nile Virus: a new invader of the western hemisphere. *Annu Rev Microbiol* **56:** 371–402.

Chu JJ, Ng ML (2002). Infection of polarized epithelial cells with flavivirus West Nile: polarized entry and egress of virus occur through the apical surface. *J Gen Virol* **83:** 2427–2435.

Dinter A, Berger EG (1998). Golgi-disturbing agents. *Histochem Cell Biol* **109:** 571–590.

Elshuber S, Allison SL, Heinz FX, Mandl CW (2003). Cleavage of protein prM is necessary for infection of BHK-21 cells by tick-borne encephalitis virus. *J Gen Virol* **84:** 183–191.

Greene LA, Tischler AS (1976). Establishment of a noradrenergic clonal line of rat adrenal pheochromocytoma cells which respond to nerve growth factor. *Proc Natl Acad Sci U S A* **73:** 2424–2428.

Gromeier M, Wimmer E (1998). Mechanism of injury-provoked poliomyelitis. *J Virol* **72:** 5056–5060.

He RT, Innis BL, Nisalak A, Usawattanakul W, Wang S, Kalayanarooj S, Anderson R (1995). Antibodies that block virus attachment to Vero cells are a major component of the human neutralizing antibody response against dengue virus type 2. *J Med Virol* **45:** 451–461.

Jordan MA, Thrower D, Wilson L (1992). Effects of vinblastine, podophyllotoxin and nocodazole on mitotic spindles. Implications for the role of microtubule dynamics in mitosis. *J Cell Sci* **102(Pt 3):** 401–416.

Lanciotti RS, Ebel GD, Deubel V, Kerst AJ, Murri S, Meyer R, Bowen M, McKinney N, Morrill WE, Crabtree MB, Kramer LD, Roehrig JT (2002). Complete genome sequences and phylogenetic analysis of West Nile virus strains isolated from the United States, Europe, and the Middle East. *Virology* **298:** 96–105.

Lanciotti RS, Roehrig JT, Deubel V, Smith J, Parker M, Steele K, Crise B, Volpe KE, Crabtree MB, Scherret JH, Hall RA, MacKenzie JS, Cropp CB, Panigrahy B, Ostlund E,

Schmitt B, Malkinson M, Banet C, Weissman J, Komar N, Savage HM, Stone W, McNamara T, Gubler DJ (1999). Origin of the West Nile virus responsible for an outbreak of encephalitis in the northeastern United States. *Science* **286:** 2333–2337.

Mabit H, Nakano MY, Prank U, Saam B, Dohner K, Sodeik B, Greber UF (2002). Intact microtubules support adenovirus and herpes simplex virus infections. *J Virol* **76:** 9962–9971.

Mackenzie JM, Jones MK, Westaway EG (1999). Markers for trans-Golgi membranes and the intermediate compartment localize to induced membranes with distinct replication functions in flavivirus-infected cells. *J Virol* **73:** 9555–9567.

Mackenzie JM, Westaway EG (2001). Assembly and maturation of the flavivirus Kunjin virus appear to occur in the rough endoplasmic reticulum and along the secretory pathway, respectively. *J Virol* **75:** 10787–10799.

Monath TP, Cropp CB, Harrison AK (1983). Mode of entry of a neurotropic arbovirus into the central nervous system. Reinvestigation of an old controversy. *Lab Invest* **48:** 399–410.

Moss B, Ward BM (2001). High-speed mass transit for poxviruses on microtubules. *Nat Cell Biol* **3:** E245–E246.

Nash D, Mostashari F, Fine A, Miller J, O'Leary D, Murray K, Huang A, Rosenberg A, Greenberg A, Sherman M, Wong S, Layton M (2001). The outbreak of West Nile virus infection in the New York City area in 1999. *N Engl J Med* **344:** 1807–1814.

O'Leary DR, Marfin AA, Montgomery SP, Kipp AM, Lehman JA, Biggerstaff BJ, Elko VL, Collins PD, Jones JE, Campbell GL (2004). The epidemic of West Nile virus in the United States, 2002. *Vector-Borne Zoonot Dis* **4:** 61–70.

Pogodina VV, Frolova MP, Malenko GV, Fokina GI, Koreshkova GV, Kiseleva LL, Bochkova NG, Ralph NM (1983). Study on West Nile virus persistence in monkeys. *Arch Virol* **75:** 71–86.

Randolph VB, Hardy JL (1988). Establishment and characterization of St Louis encephalitis virus persistent infections in Aedes and Culex mosquito cell lines. *J Gen Virol* **69(Pt 9):** 2189–2198.

Raux H, Flamand A, Blondel D (2000). Interaction of the rabies virus P protein with the LC8 dynein light chain. *J Virol* **74:** 10212–10216.

Sampson BA, Armbrustmacher V (2001). West Nile encephalitis: the neuropathology of four fatalities. *Ann N Y Acad Sci* **951:** 172–178.

Sejvar JJ, Haddad MB, Tierney BC, Campbell GL, Marfin AA, Van Gerpen JA, Fleischauer A, Leis AA, Stokic DS, Petersen LR (2003). Neurologic manifestations and outcome of West Nile virus infection. *JAMA* **290:** 511–515.

Shrestha B, Gottlieb D, Diamond MS (2003). Infection and injury of neurons by West Nile encephalitis virus. *J Virol* **77:** 13203–13213.

Smith R, Wilcox C (1996). Studies of herpes simplex virus 1 latency using primary neuronal cultures of dorsal root ganglion neurons. In: *Protocols for gene transfer in neuroscience: Towards gene therapy of neurological disorders*. Lowenstein PR, Enquist LW (eds). West Sussex, UK: John Wiley & Sons, pp 221–231.

Smithburn K, Hughes T, Burke A (1940). A neurotropic virus isolated from the blood of a native of Uganda. *Am J Trop Med Hyg* **20:** 471–492.

Solomon T, Willison H (2003). Infectious causes of acute flaccid paralysis. *Curr Opin Infect Dis* **16:** 375–381.

Sreenivasan V, Ng KL, Ng ML (1993). Brefeldin A affects West Nile virus replication in Vero cells but not C6/36 cells. *J Virol Methods* **45:** 1–17.

Stadler K, Allison SL, Schalich J, Heinz FX (1997). Proteolytic activation of tick-borne encephalitis virus by furin. *J Virol* **71:** 8475–8481.

Vasquez RJ, Howell B, Yvon AM, Wadsworth P, Cassimeris L (1997). Nanomolar concentrations of nocodazole alter microtubule dynamic instability in vivo and in vitro. *Mol Biol Cell* **8:** 973–985.

Vetterlein M, Niapir M, Ellinger A, Neumuller J, Pavelka M (2003). Brefeldin A-regulated retrograde transport into the endoplasmic reticulum of internalised wheat germ agglutinin. *Histochem Cell Biol* **120:** 121–128.